Clin Transl Oncol (2016) 18:18–26
DOI 10.1007/s12094-015-1319-6

RESEARCH ARTICLE

Endostatin exerts radiosensitizing effect in non-small cell lung cancer cells by inhibiting VEGFR2 expression

L. Liu[1] · Y. Qiao[2] · C. Hu[2] · Y. Liu[1] · Y. Xia[2] · L. Wang[2] · B. Liu[1] · H. Chen[1] · X. Jiang[2]

Received: 11 March 2015 / Accepted: 2 June 2015 / Published online: 5 November 2015

Abstract
Background To determine the effects of endostatin on vascular growth factor receptor 2 (VEGFR2) expression in non-small cell lung cancer (NSCLC) cells and the mechanisms underlying its radiosensitizing effect.
Methods VEGFR2 mRNA levels were determined in different NSCLC cell lines using qRT-PCR. RT-PCR and Western blot assays were used to assess the expression of mRNA and proteins. The radiosensitivity of the cells was determined by colony-formation assays; and cell apoptosis and cell cycle distribution were determined by flow cytometry.
Results VEGFR2 mRNA levels differed among the five NSCLC cell lines ($P < 0.01$), with the highest expression in Calu-1 cells and lowest in A549 cells. Endostatin significantly inhibited the growth of Calu-1 cells ($P < 0.01$) (IC20 = 296.5 μg/ml), and the expression of VEGFR2 and HIF-1α ($P < 0.05$). Phosphorylation of protein kinase B (Akt), extracellular signal-regulated kinases 1/2 (ERK1/2), and p38 were significantly lower in endostatin-treated cells than control ($P < 0.05$). Endostatin enhanced the radiosensitivity of Calu-1 cells to SER = 1.38 and induced apoptosis ($P < 0.01$) and G2/M blockage ($P < 0.01$). However, endostatin had limited effects on A549 cells. Compared with Calu-1 cells, there was not significantly effects on cell radiosensitivity (SER = 1.09).
Conclusions Endostatin induces apoptosis and enhances radiosensitivity of the VEGFR2 high-expressing cell line Calu-1, but it has a limited effect on the VEGFR2 low-expressing cell line A549.

Keywords Endostatin · NSCLC · VEGFR2 · HIF-1α · Radiosensitivity

Introduction

Lung cancer has the highest prevalence and mortality of any malignancy in China. Some 80 % of lung cancer cases are non-small cell lung cancer (NSCLC), with 60–70 % of patients at stages IIIB and IV at the time of diagnosis. Currently the standard treatment for localized late stage cancer is radiation therapy [1], but this therapy has limited effectiveness when used alone. Tumor relapse and distant metastasis are the main causes of radiation therapy failure [2]. For this reason, current research has focused on enhancing the radiosensitivity of tumors. Research on radiosensitizers began in the 1950s, when Langendorff first discovered that iodoacetic acid increased the death rate of mice receiving radiation [3]. Currently the major types of radiosensitizers under investigation are electrophilic radiosensitizers, biological reducers, chemodrugs, natural drugs, and molecular targeting drugs. Endostatin is one of the most frequently studied radiosensitizers. Our research group discovered that endostatin can stabilize tumor blood vessels and reduce the rate of tumor hypoxia. When it was combined with radiation therapy in the treatment of hypoxia NSCLC, it improved short-term efficacy and local control [4]. However, the mechanism by which endostatin

L. Liu, Y. Qiao and C. Hu contributed equally to this work.

✉ X. Jiang
jxdysy1970@163.com

[1] Xuzhou Medical College Graduate Academy, Xuzhou 221006, China

[2] Department of Radiation Oncology, Lianyungang First People's Hospital, No. 182, Tongguan Road, Lianyungang 222002, Jiangsu, China

enhances the radiosensitivity of tumors is still not fully understood.

In one of our previous studies, "Endostatin and radiation combination therapy of NSCLC brain metastasis phase II clinical study (NCT01410370)," we discovered that this combination therapy had good short-term efficacy, especially in patients whose primary lesions were VEGFR2-positive [5]. Recent studies have reported that VEGFR2 is expressed not only in endothelial cells but also in malignant tumor cells, such as NSCLC and breast cancer cells [6, 7]. Patients with tumors expressing high levels of VEGFR2 had shorter progression-free survival (PFS) and overall survival (OS) than those with tumors expressing little VEGFR2 [5]. This collectively suggests that poor prognosis may be caused by high levels of VEGFR2 in the tumor cells.

Previous studies have demonstrated that hypoxia-inducible factor 1α (HIF-1α) can induce radioresistance by activating related signaling pathways [8]. Yang et al. used siRNA to knock down the KDR gene in vitro and HIF-1α expression was significantly decreased [9]. However, the manner in which VEGFR2 regulates HIF-1α is still not known. Gregg et al. have shown that, under normoxic conditions, HIF-1α expression was controlled by PI3 K/Akt and MAPK/ERK pathways [10]. However, it is still not clear whether VEGFR2 regulates HIF-1α expression through these two pathways.

Here we hypothesize that tumor cells expressing VEGFR2 become resistant to radiation, probably because when VEGFR2 is activated by VEGF, it activates PI3 K/Akt and MAPK pathways, which upregulate HIF-1α expression under normoxic conditions. To test this hypothesis, we treated tumor cells in vitro with endostatin to study the role of VEGFR2 in the regulation of tumor cell radiosensitivity and the associated mechanisms.

Methods

Cell lines

The human pulmonary mucoepidermoid carcinoma (lymph node metastasis) cell line NCI-H292, human lung adenocarcinoma (lymph node metastasis) cell line NCI-H1299, human lung adenocarcinoma cell line A549, human giant-cell lung carcinoma high metastatic cell line 95D, and human lung squamous cell carcinoma cell line Calu-1 were all purchased from the Shanghai Institutes for Biological Sciences, Chinese Academy of Sciences.

Major reagents and equipment

Recombinant human endostatin (Endostar) was provided by Simcere Maidejin (Shandong, China). McCoy′s 5a and RPMI-1640 media were purchased from Sigma (US), and fetal bovine serum (FBS) was obtained from Hangzhou Sijiqing (Zhejiang, China). The RNA extraction reagent Trizol and the SYBR Green Kit were obtained from Invitrogen (US). The reverse transcription kit was obtained from Fermentas (US). The nucleic acid and protein analyzer was purchased from Eppendorf (Germany), and the real-time fluorescence PCR system was obtained from Applied Biosystems (US). Primers were designed and synthesized by Sangon Biotech (Shanghai, China). The following primers were used: β-actin: forward 5′-GTGGACATCCGCAAAGAC-3′, reverse 5′-AAAGGGTG TAACGCAACTA-3′, and the amplification product was 302 bp; VEGFR2: forward 5′-CCGTCAAGGGAAA GACTACG-3′, reverse 5′-AGATGCTCCAAGGTCAG-GAA-3′, and the amplification product was 180 bp. Antibodies to VEGFR2, HIF-1α, Akt, ERK1/2, p38, P-VEGFR2, P-Akt, P-ERK1/2, and P-p38 were all purchased from Cell Signaling Technology (US). Protein electrophoresis and electrophoretic transferring systems were from Bio-Rad (US). Cell apoptosis and cell cycle distribution analysis kits were from Nanjing KeyGEN Biotech (Jiangsu, China). The flow cytometer was from Beckman-Coulter (US). The linear accelerator was from Siemens Primus (Germany).

Cell culture

Calu-1 cells were grown in McCoy′s 5a medium supplemented with 10 % FBS. The 95D, NCI-H292, NCI-H1299, and A549 cells were grown in RPMI-1640 medium supplemented with 10 % FBS. All cells were cultured at 37 °C in a humidified incubator with 5 % CO_2.

Real-time fluorescence quantitative PCR to measure VEGFR2 mRNA levels in cells

Cells were harvested in the log phase of growth. RNA was extracted according to the manufacturer′s instructions and then reverse-transcribed into cDNA, which was subjected to fluorescence quantitative PCR analysis. Total volume for each reaction was 20 μl, and the PCR program was as follows: 95 °C for 30 s followed by 40 cycles of 95 °C for 5 s and 57 °C (57 °C for β-actin, 53 °C for VEGFR2) for 10 s, and a final 72 °C for 30 s. This was followed by melt curve analysis. Relative expression of VEGFR2 was calculated using the 2-ΔΔCt method with β-actin as the internal reference, and the assays were repeated three times.

Cytotoxicity of endostatin on Calu-1 cells determined by CCK8 assays

Calu-1 cells were resuspended to 1×10^5 cells/ml, then plated at 100 μl/well into 96-well plates. Endostatin was

added into the wells at a final concentration of 0, 200, 500, 1000, 2000, and 2500 μg/ml. Each contained six replicate wells. After 24 or 48 h of incubation, 10 μl of CCK8 solution was added into each well and further cultured for 2 h. A plate reader was used to measure the results. Tumor cell growth inhibition rate (IR) was calculated as follows: IR = (1−absorbance of treated group/absorbance of control group) × 100 %. We chose the inhibition concentration of 20 % (IC20) for the after experiments, and the assay was repeated three times.

RT-PCR and Western blot assays

Total RNA was extracted from cells according to manufacturer′s instructions and reverse-transcribed into cDNA. Primers used for PCR were as follows: VEGFR2: forward 5′-CACCACTCAAACGCTGACAT-3′, reverse 5′-CCTCTCTCCTCTCCCGACTT-3′, and the product was 310 bp; HIF-1α: forward 5′-CCCTTCAACAAACAGAATGTG-3′, reverse 5′-AGCGGTGGGTAATGGAGAC-3′, and the product was 311 bp; Akt: forward 5′-GGCACCTTCATTGGCTACAA-3′, reverse 5′-GGGACACCTCCATCTCTTCA-3′, and the product was 316 bp; ERK1: forward 5′-GGGAGGTGGAGATGGTGAAG-3′, reverse 5′-AGCAGGTTGGAGGGCTTTAG-3′, and the product was 422 bp; ERK2: forward 5′-ATTCCAAGGGCTACACCAAG-3′, reverse 5′-GCCTGTTCTACTTCAATCCTCTT-3′, and the product was 319 bp; p38: forward 5′-GACCATTTCAGTCCATCATTCA-3′, reverse 5′-GCTCACAGTCTTCATTCACAGC-3′, and the product was 321 bp in size; GAPDH: forward 5′-AGAAGGCTGGGGCTCATTTG-3′, reverse 5′-AGGGGCCATCCACAGTCTTC-3′, and the product was 258 bp in size. The PCR program was as follows: 94 °C for 10 min followed by 35 cycles of 94 °C for 30 s and 58 °C for 30 s, and a final 72 °C for 30 s.

For Western blot analysis, total protein was extracted from cells with RIPA buffer (supplemented with PMSF protease inhibitors and phosphatase inhibitors), denatured by boiling, and separated by electrophoresis. Proteins were then transferred onto membranes by the immersion method. Membranes were blocked with 5 % BSA for 1 h, and then incubated with the primary antibodies (1:1000) overnight at 4 °C. The membranes were then washed three times with PBST (10 min each), incubated with secondary antibodies (1:1000) for 1 h at room temperature, and washed again with PBS. DAB was used for color development. The assays were repeated three times.

Flow cytometry analysis of cell apoptosis

24 h after treatment, cells were washed twice with cold PBS, dissociated with EDTA-free trypsin solution, and rewashed twice with PBS (cells were centrifuged at 1500 rpm for 5 min after each wash). The supernatant was removed after the final wash, and cells were resuspended in 100 μl Annexin V-FITC binding buffer, and then 5 μl of Annexin V-FITC and PI were added to stain the cells at 4 °C in the dark for 30 min, after which 400 μl of binding buffer was added and cells were analyzed by flow cytometry.

Cell cycle analysis

Treatment as before, cells were dissociated with trypsin, washed twice with PBS, and fixed with cold 70 % ethanol at 4 °C for 24 h. Fixed cells were washed with PBS once, treated with 100 μl RNase at 37 °C for 30 min, and collected by centrifugation. Cells were incubated with 400 μl of PI solution at 4 °C for 30 min in the dark and then analyzed by flow cytometry. This experiment was performed three times.

Colony-formation assay

A pre-designated number of Calu-1 cells (10^2–10^3 cells/well) were plated into 6-well plates and were divided into three groups: control, radiotherapy, and combination therapy. Each group was evaluated in three identical wells. Cells in the combination therapy group were treated with endostatin at IC20 for 24 h and then irradiated with X-ray at room temperature at a dose of 0, 2, 4, 6, or 8 Gy. Cells were further cultured for 10–14 days. Cells were fixed and stained briefly with Giemsa according to the manufacturer′s instructions. The number of cell colonies with a diameter ≥0.2 mm was determined. The colony forming rate was calculated as the number of colonies/number of plated cells × 100 %. This experiment was performed three times.

Statistical analysis

Statistical analysis was performed with SPSS 16.0. All data are represented as mean ± standard deviation ($\bar{x} \pm s$). Comparison of the means of multiple samples was performed with single factor analysis of variance; comparison between two groups was conducted with the two sample t test; correlation analysis was conducted with two-factor correlation analysis. $P < 0.05$ was designated as statistically significant.

Results

VEGFR2 mRNA expression differed among different NSCLC cell lines

VEGFR2 mRNA levels were significantly different among these cell lines ($P < 0.01$). Relative mRNA expression of

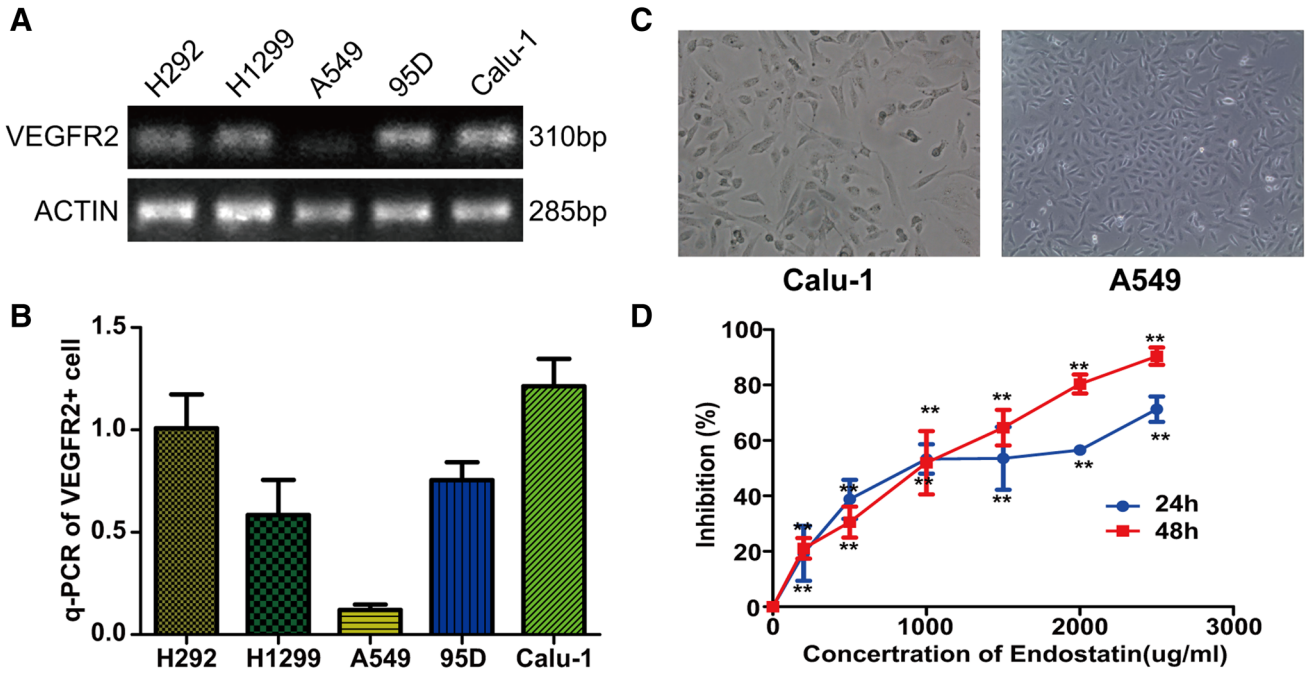

Fig. 1 Differential expression of VEGFR2 mRNA in different non-small cell lung cancer (NSCLC) cell lines. **a** VEGFR2 mRNA level was detected by RT-PCR. Various NSCLC cell lines expressed VEGFR2 at different levels ($F = 592.056$, $P < 0.01$). **b** Quantitative analysis of VEGFR2 mRNA by real-time PCR confirmed the differential expression of VEGFR2 in different cell lines ($F = 31.875$, $P < 0.01$). The level of expression was the highest in Calu-1 cells and lowest in A549 cells. **c** Calu-1 and A549 cells under normal culture conditions. **d** The death rate of Calu-1 cell by endostatin

VEGFR2 in Calu-1, NCI-H292, 95D, NCI-H1129, and A549 cells were, respectively, 1.213 ± 0.134, 1.008 ± 0.164, 0.754 ± 0.088, 0.582 ± 0.171, and 0.121 ± 0.026 (Fig. 1a, b). Calu-1 cells expressed the highest level of VEGFR2, and A549 cells expressed the lowest level of VEGFR2. The mRNA levels of VEGFR2 were not significantly different between Calu-1 and NCI-H292 cells ($P > 0.05$) or between NCI-H1299 and 95D cells ($P > 0.05$).

Endostatin promoted the death rate of Calu-1 cell

When cells were treated with different concentrations of endostatin for 24 h, the number of cell death was found increased in a dose-dependent manner (Fig. 1d). When calculated, the IC20 of endostatin after 24 and 48 h were, respectively, 296.5 and 300.5 μg/ml, between which, there was little difference. So we chose the 296.5 ug/ml concentration for 24 h in the following experiments.

Endostatin inhibited the expression of VEGFR2 and its downstream target genes

VEGFR2 and HIF-1α mRNA expression was inhibited by endostatin (Fig. 2a), and inhibition peaked after 9 h of endostatin treatment ($P < 0.01$). VEGFR2 and HIF-1α protein levels were also downregulated by endostatin (Fig. 2b), and they reached their lowest levels after 24 h of endostatin treatment ($P < 0.01$).

Molecules associated with relevant signaling pathways were evaluated. Endostatin also inhibited the expression of ERK1 and ERK2 ($P < 0.01$) but not that of Akt or p38 ($P > 0.05$) (Fig. 2c). However, endostatin did not significantly alter the total protein levels of Akt, ERK1/2, or p38 (Fig. 2d, $P > 0.05$). The level of phosphorylation of these

Fig. 2 Endostatin inhibited VEGFR2 gene expression and protein synthesis, and blocked the phosphorylation of its downstream signaling pathway proteins. Calu-1 cells were pre-treated with 296.5 μg/ml endostatin for 6, 9, or 24 h, and then stimulated with 20 ng/ml of VEGF for 6 h. Cells were then collected for RT-PCR and Western blot assays. **a** RT-PCR results showed that VEGFR2 mRNA expression increased significantly upon VEGF stimulation ($P < 0.01$) and that endostatin inhibited the VEGF-induced expression of VEGFR2 mRNA ($F = 66.728$, $P < 0.01$) and of HIF-1α mRNA. The greatest inhibition occurred with 9 h of endostatin pre-treatment ($P < 0.01$). **b** Western blot analysis showed that VEGFR2 protein levels increased upon VEGF stimulation ($P = 0.012$), but endostatin pre-treatment decreased protein levels of VEGFR2 and HIF-1α ($P < 0.05$). The most significant inhibitory effect was seen after 24 h of endostatin pre-treatment ($P < 0.01$). **c** Blocking VEGFR2 did not significantly alter gene expression of Akt, ERK1/2, or p38 ($P > 0.05$). **d** Similarly, endostatin did not significantly change the total protein levels of Akt, ERK1/2, or p38 ($P > 0.05$). **e** Endostatin inhibited the phosphorylation of Akt, ERK1/2, and p38 ($P < 0.05$) (*$P < 0.05$, **$P < 0.01$, compared with control)

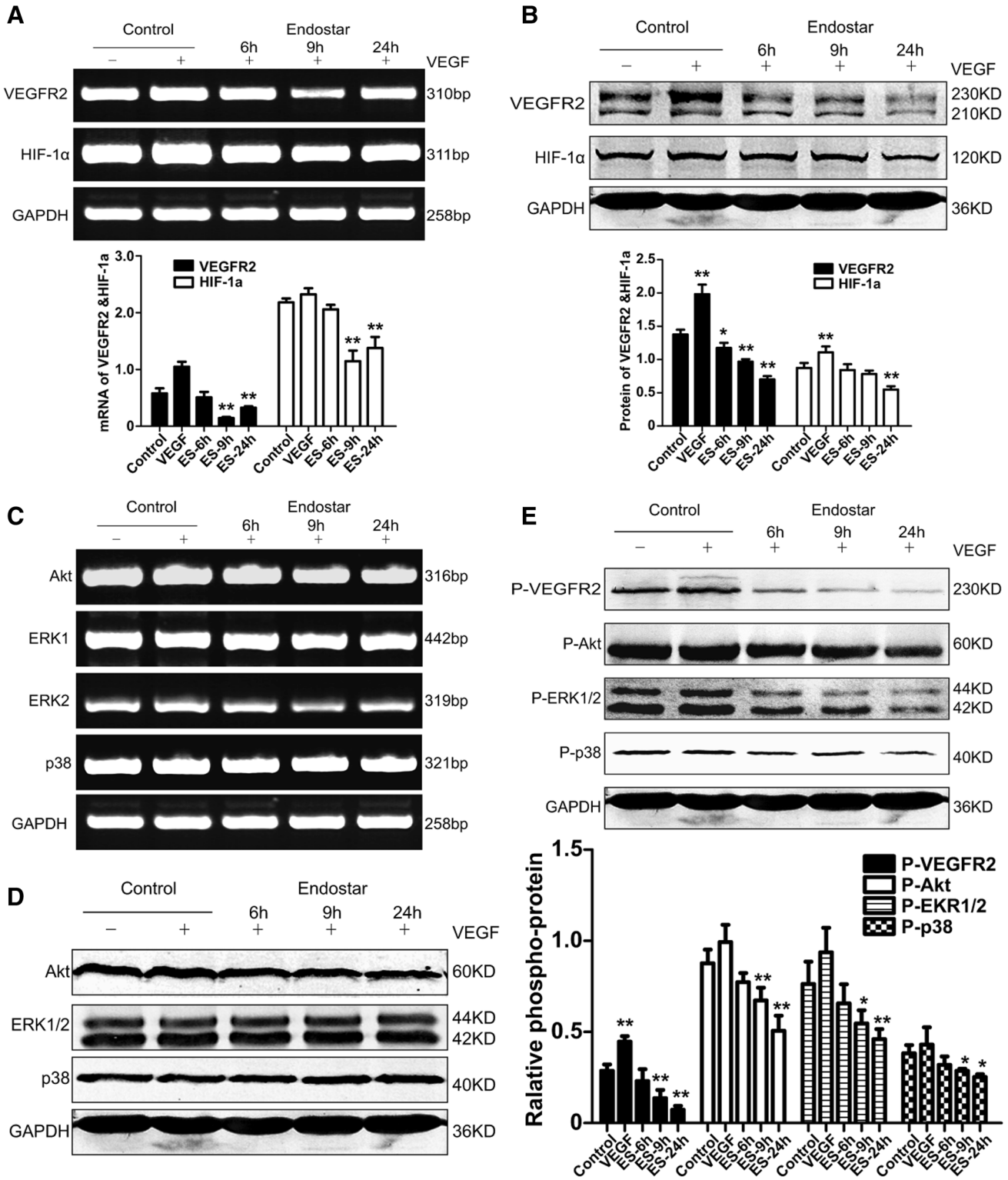
A
Control
Endostar
6h
9h
24h
VEGF
VEGFR2
310bp
HIF-1α
311bp
GAPDH
258bp
mRNA of VEGFR2 &HIF-1a
VEGFR2
HIF-1a
Control
VEGF
ES-6h
ES-9h
ES-24h
B
230KD
210KD
120KD
36KD
Protein of VEGFR2 &HIF-1a
C
Akt
316bp
ERK1
442bp
ERK2
319bp
p38
321bp
D
60KD
ERK1/2
44KD
42KD
40KD
E
P-VEGFR2
230KD
P-Akt
60KD
P-ERK1/2
44KD
42KD
P-p38
40KD
Ralative phospho-protein
P-VEGFR2
P-Akt
P-EKR1/2
P-p38

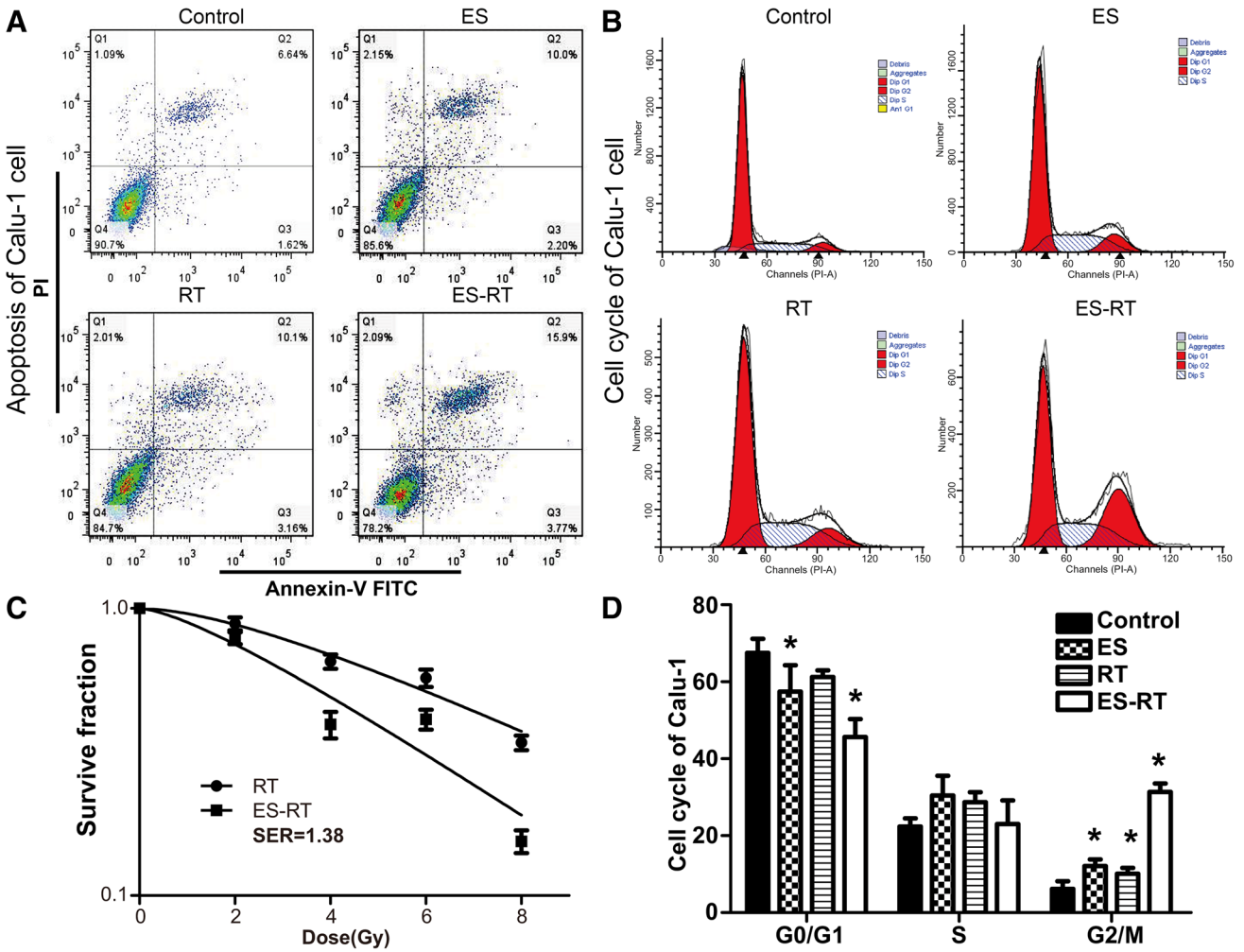

Fig. 3 Endostatin promoted apoptosis, enhanced radiosensitivity, and changed the cell cycle distribution of Calu-1 cells. Cells were divided into control, drug only, radiation only, and combined treatment groups. The control cells were left untreated; drug-only cells were treated with 296.5 μg/ml of endostatin, and radiation-only cells were irradiated by 2 Gy. All treated groups were then cultured for 24 h. Combined treatment cells were then pre-treated with endostatin for 24 h, irradiated by 2 Gy, and then cultured for a further 24 h. Apoptosis and cell cycle distribution were analyzed by flow cytometry. For the colony-formation assay, cells were divided into control, radiation only, and combined treatment groups. Cells in each group were treated as described above. **a** Endostatin-induced apoptosis of Calu-1 cells, and further enhanced radiation-induced Calu-1 cell apoptosis ($F = 44.153$, $P < 0.01$). **b**, **d** The number of Calu-1 cells in the G2/M phase were increased with endostatin treatment ($P < 0.01$). **c** Endostatin enhanced radiosensitivity of Calu-1 cells (SER = 1.38) (*$P < 0.05$, **$P < 0.01$, compared with control)

proteins was then assessed. Endostatin inhibited the phosphorylation of VEGFR2, Akt, ERK1/2, and p38 to various degrees (Fig. 2e). This inhibitory effect peaked after 24 h of endostatin treatment ($P < 0.01$).

Endostatin and radiation combination therapy affected apoptosis, cell cycle progression, and radiosensitivity of Calu-1 cells

24 h of endostatin treatment induced cell apoptosis in Calu-1 cells ($P < 0.01$). With 2 Gy irradiation, apoptosis was increased in the combination therapy group than the radiation-only group ($P < 0.01$) (Fig. 3a). Cell cycle analysis showed that, with endostatin treatment, more Calu-1 cells appeared in G2/M phase (Fig. 3b, $P < 0.05$). The combined treatment group showed the greatest increase of cells in the G2/M phase and was significantly different from the control group ($P < 0.01$). The cell survival curve of the combined treatment group was lower than that of the group treated with radiation alone, with a sensitivity enhancement ratio (SER) of 1.38.

Endostatin enhanced the radiosensitivity of Calu-1 cells, but not A549 cells

To determine whether endostatin is effective on VEGFR2-low-expressing cells, the responses of A549 cells to endostatin were compared to those of Calu-1 cells.

VEGFR2 mRNA levels were nearly undetectable in A549 cells (Fig. 4a), and a very low protein level was detected by Western blot analysis (Fig. 4b). Unlike Calu-1 cells, endostatin treatment did not affect HIF-1α protein levels in A549 cells ($P > 0.05$). In addition, endostatin treatment did not affect either apoptosis or cell cycle progression in A549 cells ($P > 0.05$). Cell survival curves of A549 cells of the combination therapy group were not significantly different from those of the radiation-alone group, with a SER of 1.09 (Fig. 4e).

Discussion

Radiation therapy alone is not very effective in NSCLC patients, largely due to the radioresistance of the cancer cells. Radiosensitizers have been widely used clinically to improve the effectiveness of radiation therapy. Endostatin is one such radiosensitizer. This study demonstrates that endostatin enhances the radiosensitivity of the VEGFR2 high-expressing Calu-1 cells. The mechanism of this effect probably involves downregulation of VEGFR2 expression, which in turn downregulates HIF-1α expression through two non-hypoxia pathways, the PI3 K/Akt and MAPK pathways.

Many studies have shown that VEGF-A is an important growth factor that promotes angiogenesis. VEGFR2 is the main functional receptor of VEGF-A on endothelial cells, playing pivotal roles in transducing VEGF-A signaling. When activated by VEGF, VEGFR2 enhances blood vessel permeability and induces endothelial cell proliferation and migration [11]. Recent studies have indicated that VEGFR2 is expressed not only in endothelial cells, but also on tumor cells [6, 7]. It has been proposed that VEGFR2 expression may be an independent malignant phenotype of NSCLC [9]. Kim et al. used an enzyme-linked immunoabsorption assay and showed that endostatin did not neutralize VEGF but rather bound directly to the extracellular domain of VEGFR2 on the surface of endothelial cells, so preventing the binding of VEGF to VEGFR2 and the subsequent formation of VEGFR2 homodimers and their autophosphorylation [12]. Our study showed that VEGFR2 mRNA was expressed in human NSCLC cells cultured in vitro, but its levels varied significantly across different cell lines. And endostatin treatment was associated with decreases in VEGFR2 expression at both the mRNA and protein levels, and its protein phosphorylation level was also reduced, suggesting that endostatin acts by directly inhibiting VEGFR2 expression and activation. When VEGFR2 expression was reduced, Calu-1 cells exhibited increased apoptosis and disrupted cell cycle progression with cells accumulating in the G2/M phase and increased radiosensitivity (SER = 1.38). However, A549 cells, which express low levels of VEGFR2, did not show enhanced radiosensitivity upon endostatin treatment (SER = 1.09), suggesting that endostatin has limited radiosensitizing effect on tumors expressing low levels of VEGFR2. The heterogeneous effect of endostatin observed clinically may be due to variable levels of VEGFR2 in patients′ tumors. In this way, the current study provides a theoretical basis for improving the therapeutic effects of endostatin, suggesting that endostatin should be primarily used in patients whose tumors express high levels of VEGFR2.

There is some question regarding the mechanism that mediates the radiosensitizing effect of endostatin downstream of its inhibition of VEGFR2 expression. Earlier studies have shown that HIF-1α is a transcription factor that is widely expressed in mammalian and human tissues under hypoxic conditions. It binds to hypoxia-inducible elements to activate the transcription of many downstream genes, including VEGF, erythropoietin (EPO), and glycolytic enzymes, thereby promoting tumor invasion and radioresistance [13]. Meijer et al. found that inhibiting HIF-1α expression in tumor cells enhanced their radiosensitivity [14]. The connection between VEGFR2 and HIF-1α was also examined. Here we found that when VEGFR2 was downregulated by endostatin, HIF-1α expression was inhibited at both the mRNA and protein levels, and this inhibition was positively correlated with the changes in VEGFR2 expression ($r_p = 0.779$, $P = 0.001$), suggesting that VEGFR2 signaling regulates HIF-1α expression. Agani et al. found that, under normoxic conditions, HIF-1α expression in tumors was induced by insulin, insulin-like growth factors (IGFs), epithelial growth factor (EGF), and interlukin (IL)-1 through the PI3 K pathway [15]. These ligands bind to and activate their respective tyrosine kinase receptors, which in turn activate PI3 K, Akt, and mTOR, and subsequently mTOR upregulates HIF-1α protein levels in cells. The mitogen-activated protein kinase (MAPK) family includes three main categories: ERK1/2, p38 MAPK, and c-Jun N-terminal kinases/stress-activated protein kinases. In vivo and in vitro studies have found that ERK1/2 and p38 MAPK can directly phosphorylate HIF-1α, augmenting its transcriptional activity [16, 17]. Results also showed that ERK1/2 promotes the phosphorylation of p300/CBP and its binding to HIF-1α, thus indirectly inducing HIF-1α activation [18]. Our results showed that VEGF stimulation phosphorylated and activated VEGFR2 and its downstream signaling molecules Akt, ERK1/2, and p38; endostatin treatment blocked VEGFR2 activation, leading to deactivation of Akt, ERK1/2, and p38. These data suggest that activated VEGFR2 promotes HIF-1α expression through PI3 K/Akt and MAPK/ERK pathways. However, in A549 cells that express low levels of VEGFR2, HIF-1α is still

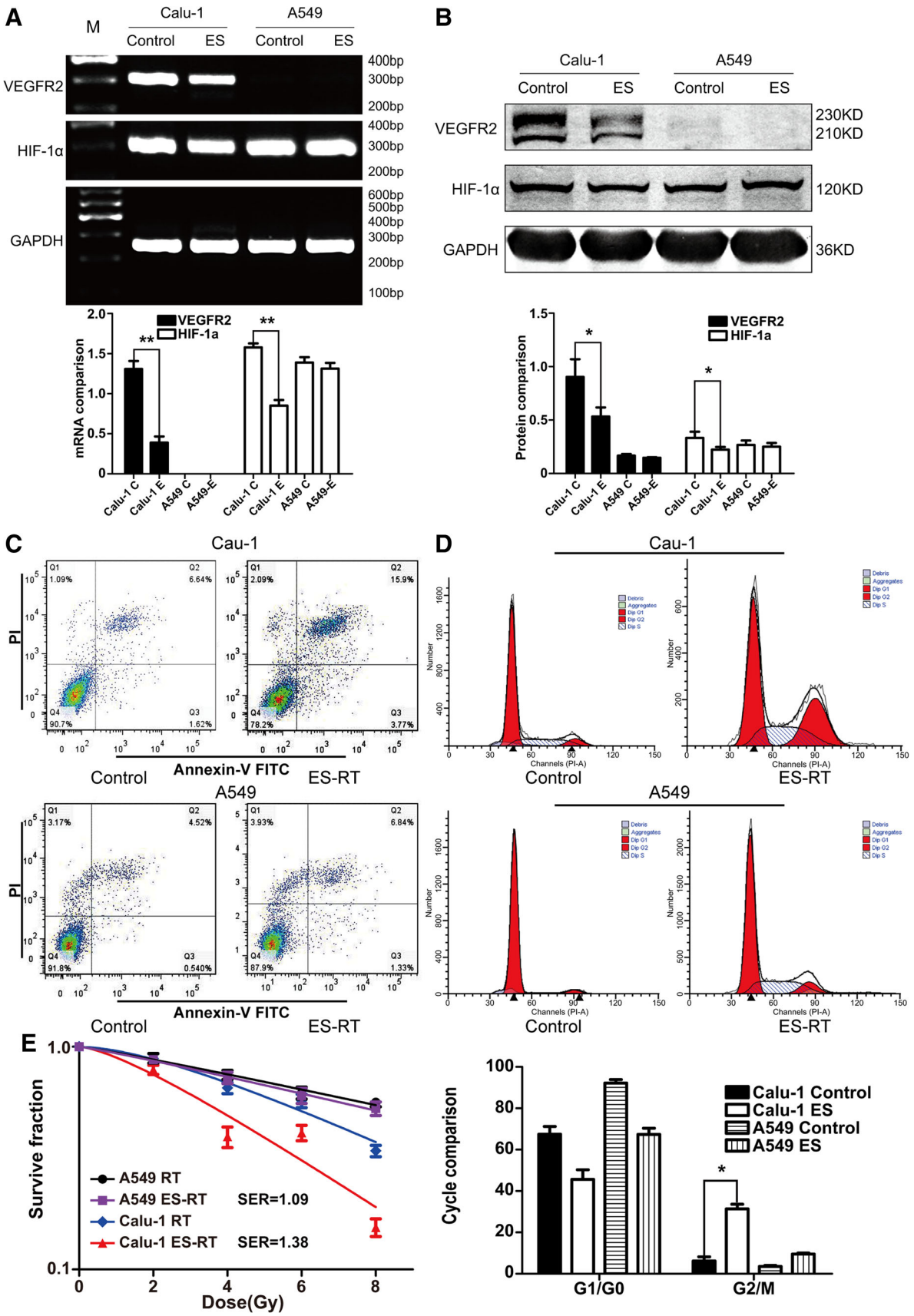
A
M
Calu-1
A549
Control
ES
Control
ES
VEGFR2
HIF-1α
GAPDH
400bp
300bp
200bp
400bp
300bp
200bp
600bp
500bp
400bp
300bp
200bp
100bp
mRNA comparison
VEGFR2
HIF-1a
**
**
Calu-1 C
Calu-1 E
A549 C
A549-E
B
Calu-1
A549
Control
ES
Control
ES
VEGFR2
HIF-1α
GAPDH
230KD
210KD
120KD
36KD
Protein comparison
VEGFR2
HIF-1a
*
*
C
Cau-1
PI
Annexin-V FITC
Control
ES-RT
A549
D
Cau-1
Number
Channels (PI-A)
Control
ES-RT
A549
E
Survive fraction
A549 RT
A549 ES-RT
SER=1.09
Calu-1 RT
Calu-1 ES-RT
SER=1.38
Dose(Gy)
Cycle comparison
Calu-1 Control
Calu-1 ES
A549 Control
A549 ES
*
G1/G0
G2/M

◀**Fig. 4** Endostatin had no effect on apoptosis, cell cycle progression, or radiosensitivity in A549 cells. A549 cells were compared to Calu-1 cells in their responses to endostatin. Cells in control and drug-only groups (as in Fig. 3) were used in RT-PCR and Western blot assays. Cells in control and combined treatment groups (as in Fig. 3) were used in flow cytometric analysis of apoptosis and cell cycle distribution. Colony-formation assays were performed as in Fig. 3. **a** VEGFR2 mRNA level in A549 cells was nearly undetectable by RT-PCR. **b** The inhibitory effect of endostatin on the protein levels of VEGFR2 and HIF-1α was not significant ($P = 0.315$, $P = 0.628$). **c** The apoptosis-inducing effect of endostatin was more pronounced in Calu-1 cells than in A549 cells. **d** Endostatin had a more pronounced effect on G2/M phase cell accumulation in Calu-1 cells than in A549 cells. **e** Endostatin enhanced radiosensitivity of Calu-1 cells but not that of A549 cells (SER = 1.09) ($^*P < 0.05$, $^{**}P < 0.01$, compared with control)

expressed at high levels, presumably through VEGFR2-independent pathways. As mentioned earlier, IGFs, EGF, IL-1 can stimulate HIF-1α expression [15]. In addition, Nilsson et al. reported that, under normoxic conditions, activation of receptor tyrosine kinases (RTKs), such as VEGFR1, PDGFR-β, and EGFR increased HIF-1α levels [19]. In this way, the high levels of expression of HIF-1α in A549 cells may have been caused by some of these mechanisms.

In summary, the current work shows that in tumor cells expressing high levels of VEGFR2 mRNA, and its probable mechanism is that VEGFR2 activates HIF-1α expression through PI3 K and MAPK/ERK pathways, leading to radioresistance. Endostatin inhibits the activation of VEGFR2, thereby downregulating HIF-1α expression, enhancing the radiosensitivity of tumor cells, and improving the efficacy of radiation therapy. This study thus provides a theoretical basis for the clinical use of endostatin in combination with radiotherapy in anti-tumor therapies.

Acknowledgments This study was supported by the National Natural Science Foundation of China (NO. 81472792), Research Fund from Ministry of Health (W201210), and the National Natural Science Foundation of Jiangsu Province (BK2012661).

Conflict of interests We have read and understood *Clinical and Translational Oncology*'s policy on disclosing conflicts of interest and declare that we have none.

Ethics statement Our study did not refer to clinical trial and animal trial, so there was no ethics statement.

References

1. Yeo SG, Kim ES. Efficient approach for determining four-dimensional computed tomography-based internal target volume in stereotactic radiotherapy of lung cancer[J]. Radiat Oncol J. 2013;31(4):247–51.
2. Chi A, Liao Z, Nguyen NP, Xu J, Stea B, Komaki R. Systemic review of the patterns of failure following stereotactic body radiation therapy in early-stage non-small-cell lung cancer: clinical implications. Radiother Oncol. 2010;94:1–11.
3. Langendorff H, Koch R. Studies on biological radioprotection. IX. Effect of SH-blockers on radiosensitivity. Strahlentherapie. 1954;95(4):535–41.
4. Jiang X-D, Qiao Y, Dai P, Wu J, Song D-A, Li S-Q, et al. Preliminary clinical study of weekly recombinant human endostatin as a hypoxic tumour cell radiosensitiser combined with radiotherapy in the treatment of NSCLC. Clin Transl Oncol. 2012;14(6):465–70.
5. Jiang X-D, Ding M-H, Qiao Y, Liu Y, Liu L. Study on lung cancer cells expressing VEGFR2 and the impact on the effect of RHES combined with radiotherapy in the treatment of brain metastases. Clin Lung Cancer. 2014;15(2):e23–9.
6. Donnem T, Al-Shibli K, Andersen S, Al-Saad S, Busund L-T, Bremnes RM. Combination of low vascular endothelial growth factor A (VEGF-A)/VEGF receptor 2 expression and high lymphocyte infiltration is a strong and independent favorable prognostic factor in patients with nonsmall cell lung cancer. Cancer. 2010;116:4318–25.
7. Dhakal HP, Naume B, Synnestvedt M, Borgen E, Kaaresen R, Schlichting E, et al. Expression of vascular endothelial growth factor and vascular endothelial growth factor receptors 1 and 2 in invasive breast carcinoma: prognostic significance and relationship with markers for aggressiveness. Histopathology. 2012;61:350–64.
8. Grosso S, Doyen J, Parks SK, Bertero T, Paye A, Cardinaud B, et al. MiR-210 promotes a hypoxic phenotype and increases radioresistance in human lung cancer cell lines. Cell Death Dis. 2013;4:e544.
9. Yang F, Tang X, Riquelme E, Behrens B, Nilsson MB, Giri U, Tang X, et al. Increased VEGFR-2 gene copy is associated with chemoresistance and shorter survival in patients with non-small-cell lung carcinoma who receive adjuvant chemotherapy. Cancer Res. 2011;71(16):5512–21.
10. Semenza G. Signal transduction to hypoxia-inducible factor 1. Biochem Pharmacol. 2002;64(5–6):993–8.
11. Kerbel RS. Tumor angiogenesis. N Engl J Med. 2008;358(19):2039–49.
12. Kim Y-M, Hwang S, Kim Y-M, Pyun B-J, Kim T-Y, Lee S-T, et al. Endostatin blocks vascular endothelial growth factor-mediated signaling via direct interaction with KDR/Flk-1.[J]. J Biol Chem. 2002;277(31):27872–9.
13. Brown JM, Giaccia AJ. The unique physiology of solid tumors: opportunities(and problems)for cancer therapy[J]. Cancer Res. 1998;58(7):1408–16.
14. Meijer TWH, Kaanders JHAM, Span PN, Bussink J. Targeting hypoxia, HIF-1, and tumor glucose metabolism to improve radiotherapy efficacy. Clin Cancer Res. 2012;18(20):5585–94.
15. Agani F, Jiang B-H. Oxygen-independent regulation of HIF-1: novel involvement of PI3 K/AKT/mTOR pathway in cancer. Curr Cancer Drug Targets. 2013;13:245–51.
16. Karapetsas A, Giannakakis A, Pavlaki M, Panayiotidis M, Sandaltzopoulos R, Alex Galanis. Biochemical and molecular analysis of the interaction between ERK2 MAP kinase and hypoxia inducible factor-1α. Int J Biochem Cell Biol. 2011;43(11):1582–90.
17. Sodhi A, Montaner S, Patel V, Zohar M, Bais C, Mesri EA, et al. The Kaposi's sarcoma-associated herpes virus G protein-coupled receptor up-regulates vascular endothelial growth factor expression and secretion through mitogen-activated protein kinase and p38 pathways acting on hypoxia-inducible factor 1alpha. Cancer Res. 2000;60(17):4873–80.
18. Sang N, Stiehl DP, Bohensky J, Leshchinsky I, Srinivas V, Caro J. MAPK signaling up-regulates the activity of hypoxia-inducible factors by its effects on p300. J Biol Chem. 2003;278(16):14013–9.
19. Nilsson MB, Zage PE, Zeng L, Xu L, Cascone T, Wu HK, et al. Multiple receptor tyrosine kinases regulate HIF-1alpha and HIF-2alpha in normoxia and hypoxia in neuroblastoma: implications for antiangiogenic mechanisms of multikinase inhibitors. Oncogene. 2010;29(20):2938–49.